



Journal of Renewable Energies

Revue des Energies Renouvelables

journal home page : <https://revue.cder.dz/index.php/rer>

Triple junction solar cell with Cu In_{1-x} Ge_x Se as absorbents layers

Amina Maria Laoufi ^{a,*}, Latifa Mousli ^b, Benmoussa Dennai ^b

^a Tahri Mohamed University, Smart Grid & Renewable Energy (SGRE LAB) Bechar, Algeria.

^b Tahri Mohamed University, Laboratory for the Development of Renewable Energies and their Applications in Saharan areas (LDERAS). Bechar, Algeria.

* Corresponding author, E-mail address: laoufi.aminamaria@univ-bechar.dz

Tel.: + 2136562092

Abstract

The design of multi-junction solar cells is guided by both the theoretical optimum bandgap combinations as well as the realistic limitations to materials with these bandgaps. Nowadays, triple-junction III-V multi-junction solar cells are commonly used as GaAs, InGaAs; InGaP ... In this work, we are interested in studying triple junctions based on thin-film solar cells Cu(In_{1-x}Ga_x) Se₂, CuInSe₂, and CuGaSe₂ quaternaries using Silvaco ATLAS software. Incorporating Cu(In_{0.34}Ga_{0.66}) Se₂ as an absorber in the middle sub-cell increased the open-circuit voltage by 0.72 V. The highest cell efficiency is 20.89 % (V_{oc} = 2.33 V, J_{sc} = 9.97 mA/cm², FF = 89.62%). This triple-junction solar cell demonstrates the potential and limitations of future improvements when voltage and current are considered.

Keywords: Thin film solar cell, CGS, CIGS, CIS, tandem solar cell.

1. Introduction

There have been remarkable developments in the technology of Photovoltaic Cells [1]. There has been a surge in the development, manufacturing, and use of multi-junction solar cells all throughout. But, there were obstacles such as composition, overall size, and lattice matching of different junctions which have now almost been overcome by the use of transparent and conductive buffer layers or tunnel junctions [2-6]. Usually, an III-V multi-junction solar cell has been used as GaAs, InGaAs; InGaP.... The 3J solar cells are used due to the ease of growth. A number of Multi-junction thin film, and Si structures have been proposed. There are 5-junction cells such as AlGaInP/ AlGaInAs/GaInAs/GaInNAs/Ge solar cells which result in a decent efficiency but are difficult to fabricate due to lattice mismatching and therefore need

more tunnel junctions and buffer layers that lead to a higher number of trap levels and growth defects which lead to higher unwanted recombination [2, 7-11]. The non-radiative recombination causes the lattice to heat up which is unwanted. For that reason, in this paper, we propose a triple junction solar cell based on thin-film Cu In_{1-x} Ga_x Se.

The CIGS-based thin film solar cells have earned special interest among the thin film solar cells because of their high efficiency [12-15]. And this is not the only advantage of it. The band gap of CIGS can be varied from 1.011 to 1.67 eV in such a way by varying Ga composition to obtain the required band gap that meets the solar spectrum to absorb most of the photons [13,16-18]. As well as the thermal expansion coefficient of CIGS matches with soda-lime glass (SLG). In order to make an abrupt junction with the window layer, the carrier concentration and resistivity of CIGS can be varied by controlling its intrinsic composition without using extrinsic dopants [19].

The triple junction solar cell was presented, it is composed of Zinc oxide as a window layer for all the sub-cells, cadmium sulfide (CdS) as an emitter layer for three sub-cells, copper gallium diselenide (CGS) as the first absorber layer, copper indium gallium diselenide (CIGS) as the second absorber layer, for the third absorber is copper indium diselenide and the substrate is molybdenum.

2. Modeling and numerical simulation

Figure 1 shows the structure of CGS/CIGS/CIS tandem solar cell comprised of a wider band gap CGS top sub-cell which is monolithically integrated to a middle band gap CIGS bottom sub-cell then smaller band gap CIS in series. Emitter layers used is n-type. The absorbers have band gaps of 1.67, 1.39 and 1.011 eV for x values of 1, 0.66 and 0 respectively.

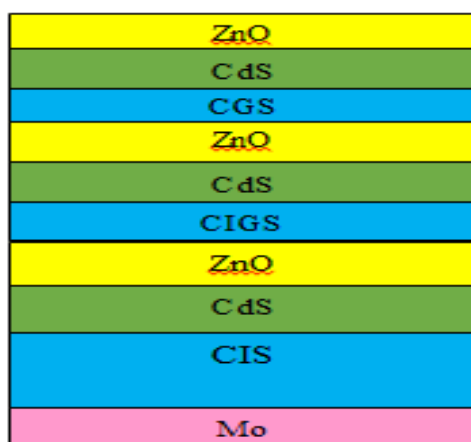


Fig.1. Silvaco-Atlas structure file of the CGS/CIGS/CIS tandem solar cell.

Cu In_{1-x}Ga_xSe₂ is a compound with a band gap energy which is dependent on composition ratio $x = \text{Ga}/(\text{Ga} + \text{In})$ and can be extracted from the relation below [14,18]:

$$E_g(x) = 1.011 + 0.664x - 0.249(1 - x) \quad (1)$$

The electron affinity of CIGS is expressed below:

$$\chi(x) = -0.242x^2 - 0.454x + 4.68 \quad (2)$$

The relative permittivity:

$$\epsilon(x) = 15.1 - 5x \quad (3)$$

Where V_{oc} is open-circuit voltage and J_{sc} is the short-circuiting current density. According to Eqs. (2) and (3) open-circuit voltage of the tandem cell equals the sum of open circuit voltages of each of the sub-cells and one sub-cell limits the current of the whole structure.

$$V_{oc,tandem} = V_{oc,top} + V_{oc,middle} + V_{oc,bottom} \quad (4)$$

$$J_{sc,tandem} = J_{sc, \min}(J_{sc,top}, J_{sc,bottom}) \quad (5)$$

In this work, the simulations were all performed AM1.5 solar spectrums with $P = 1000\text{W}/\text{cm}^2$ and at temperature $T = 300\text{ K}$ using the one diode ideal model.

Table .1 shows the description of the parameters used in the simulation and the basic parameters that are used in the study.

Table 1. Material Parameters used in the simulation

Parameters	ZnO	CdS	CGS	CIGS	CIS
Thickness (μm)	0.05	0.05	0.10	1.5	1
ϵ	9	10	10.1	13.55	15.1
E_g (eV)	3.3	2.48	1.675	1.163	1.011
χ (eV)	4.5	4.18	3.984	4.51	4.68
$\mu_n(\text{cm}^2/\text{Vs})$	100	100	100	100	100
$\mu_p(\text{cm}^2/\text{Vs})$	25	25	25	25	25
$N_c(\text{cm}^{-3})$	$2.2e^{18}$	$2.41e^{18}$	$2.2e^{18}$	$2.2e^{18}$	$2.2e^{18}$
$N_v(\text{cm}^{-3})$	$1.8e^{19}$	$2.57e^{19}$	$1.8e^{19}$	$1.8e^{19}$	$1.8e^{19}$

For the great efficiency and CIGS tandem solar cells stability, we performed this simulation; the results can be presented in the following figures. This figure demonstrates the cell parameters such as V_{OC} , J_{SC} , FF and η from SILVACO simulation.

A voltage is applied to the cell, the current lowers, and the voltage grows when the charge is construct-up up at the terminals. The owing current might be considered as the sum of the short circuit current I_{SC} , generated by the process of absorbing the photons. The current density is as follows [17-19]:

$$j = j_{sc} - j_0 \left(e^{\frac{qV}{T k_B}} - 1 \right) \quad (6)$$

With, J_0 is a constant, q is the electron charge and V is the applied voltage. By setting $J=0$ the open circuit voltage V_{OC} can be calculated:

$$V = \frac{T k_B}{qV} \ln \left(\frac{J_{sc}}{J_0} + 1 \right) \quad (7)$$

The maximum output power density of a solar cell is achieved at a voltage V_m and the corresponding current density is J_m , and thus the maximum power density is:

$$P_m = J_m * V_m \quad (8)$$

The ratio of the maximum power produced on the incident light power is the definition of the efficiency of the solar cell.

$$\eta = \frac{P_{max}}{P_{inc}} = \frac{I_{max} V_{max}}{P_{inc}} \quad (9)$$

3. Results and discussion

The results shown below are the results obtained in our work which is represented in the modelling of a triple- junction solar cell, the simulations were all performed AM1.5 solar spectrums with $P = 1000W/cm^2$ and at temperature $T= 300 K$ using the one diode ideal model. First, we simulated the solar cell without the middle sub-cell (double junction solar cell CGS/CIS). then, we added another sub-cell between them, the absorber layer is based on CIGS with band-gap equaled 1.39 eV with molar fraction $x= 0.66$. And we examined the effect of temperature on the new cell on The efficiency, the fill factor, the density current of the short circuit and the open-circuit voltage.

3.1 How to choose the middle cell?

For a total thickness of 270 nm of the cell, we calculated the short-circuit current densities, the open-circuit voltage, the shape factor and the efficiency of the cell for different values of the molar fraction of the emitter. $(Cu In_{1-x}Ga_xSe) P$ layer ranging from band gap at 1.011 eV for $x=0$ to 1.67 eV for $x = 1$ and values of 0, 0.31, 0.45, 0.66 and 1 and for CIGS thicknesses varying from 1 μm to 3 μm . The results are reported in the figures.

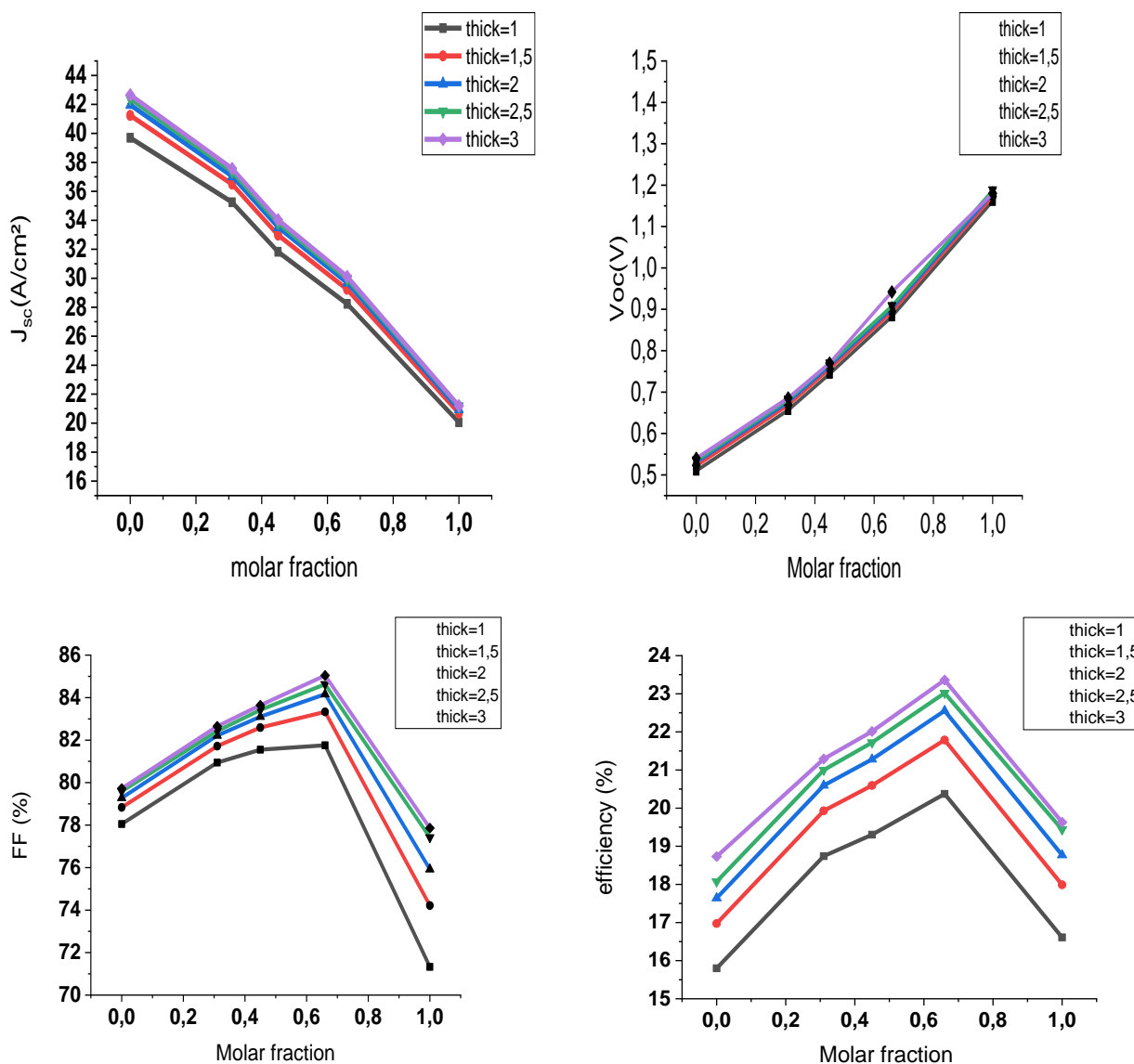


Fig.2. Influence of the molar fraction of the absorbent layer on the J_{sc} , V_{oc} , FF and η .

The photovoltaic parameters in terms of J_{sc} , V_{oc} , FF and η were simulated for CIGS thicknesses varying from 1 μm to 3 μm and the CdS thickness is constant (50 nm). An increase in these parameters is observed with the thickness of the absorbent layer. For the thickness equal to 1 μm, the yield is 20.37% at $x=0.66$. The increase in conversion efficiency is mainly due to the increase in thickness of CIGS. A possible explanation is that as the thickness increases, more photons

with longer wavelengths can be collected in the CIGS layer. Hence, it will contribute to greater generation of electron-hole pairs, which will increase short-circuit current, open-circuit voltage, and efficiency. A very thin CIGS layer physically means that the back contact and depletion region are very close. This effect further promotes electronic recombination at the rear contact. This type of recombination is detrimental to cell performance as it affects J_{sc} , V_{oc} and η .

The increase in the forbidden band increases the open circuit voltage which reaches the value 1.19 V and 1.16 . While there is a decrease in the short-circuit current due to the reduction in the number of absorbed photons. [20]

The efficiency increases with x, up to x=0.66, the yield decreases at x=1. A high Ga x composition corresponding to a high defect density causes a drop in the short-circuit current and subsequently the efficiency of the solar cell. Noting that the optimal value of efficiency 20.37% at x=0.66 corresponding to a gap energy of the order of 1.39 eV in very good agreement with these observations are in good agreement with the simulation in Silvaco. [21]

3.2 The quantum efficiency

We have first demonstrated the variation of the quantum efficiency (QE) versus wavelength for both the top and bottom cells of the tandem solar cell in Figure 3. The top tandem sub-cell has absorbed the short wavelength region below 0.74 μm , then the middle sub-cell starts to absorb the wavelength range between 0.74 and 0.89 μm and the bottom cell absorbs the remainder of the spectrum

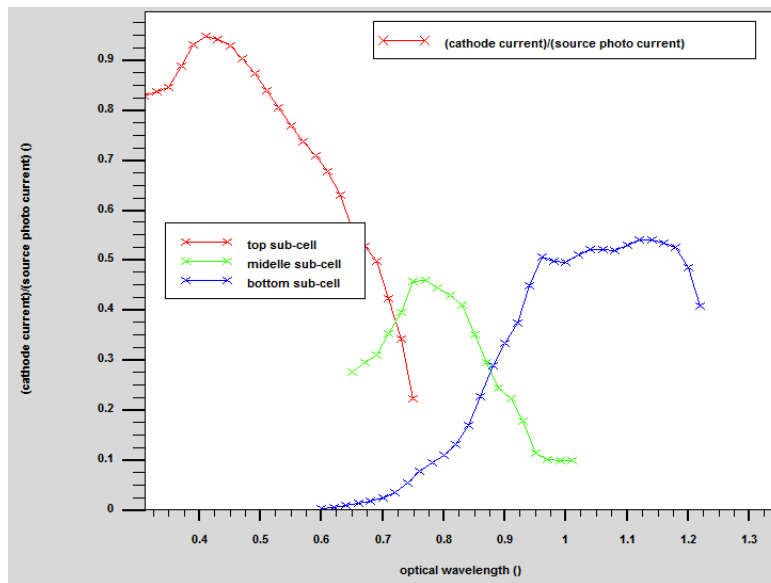


Fig.3. Quantum efficiency of sub-cells versus wave length.

3.3 Characteristic (I-V) and (P-V)

The IV curves of the devices are shown in Figure.4, measured under the global spectrum (at 300 K and 1000 W/m² irradiance), while Figure 5 represents the power-voltage (P-V) of the CGS top cell, CIGS middle and CIS bottom sub-cell, and CGS/CIGS/CIS tandem cell.

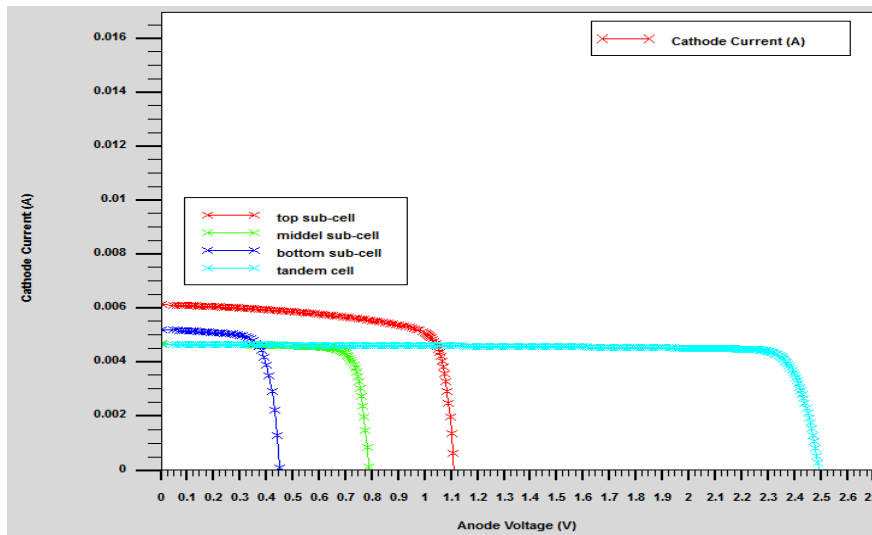


Fig.4. I-V Characteristic Overlay of CGS top, CIGS middle, CIS bottom sub- cells and Tandem cell.

As we know in the tandem solar cell the open-circuit voltage is the summation of V_{oc} of the top, middle and the bottom while the short-circuit current density is taking the lower. In this case V_{oc} is 2.49 V, as much as the sum of the CGS top (1.10 V) and the CIGS middle (0.78 V) and CIS bottom (0.45 V) sub-cells when J_{sc} is 9.33 mA/cm^2 .

Due to the convergence of the bandgaps of the sub-cells of the tandem cell, the solar spectrum has not been exploited more extensively. A solar cell of the same materials has been simulated to reduce the production cost and avoid miss-match of the material used

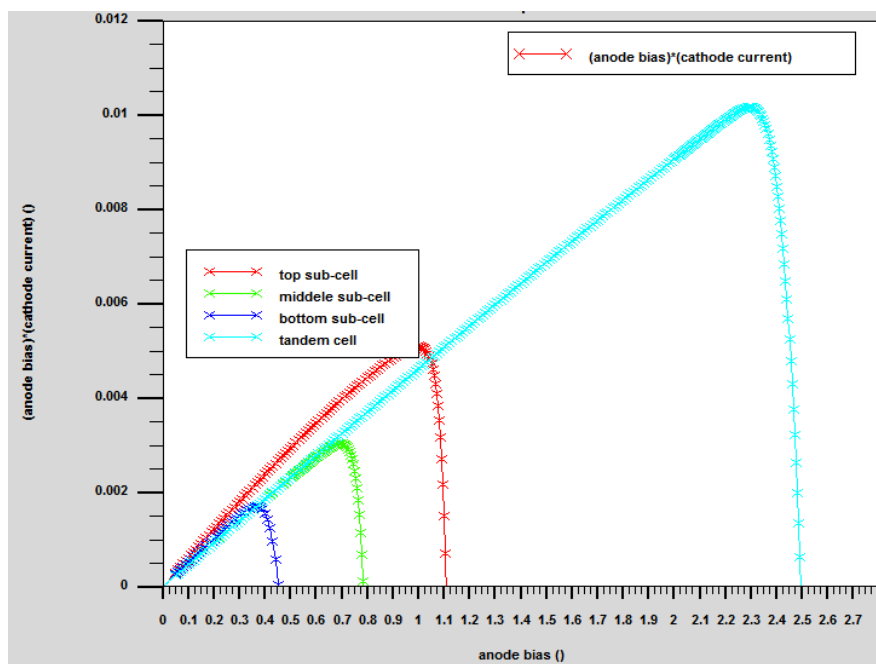


Fig.5. P-V Characteristic Overlay of CGS top, CIGS middle, CIS bottom and Tandem cell.

3.4 Characteristic (I-V) and (P-V) of the double and triple junction

We first compared the PV performance of triple-junction cells with the double junctions with the same structure without the middle sub-cell. The solar cell with triple junction exhibited a significantly higher efficiency than those with double junction. The best-performing triple junction cell showed an efficiency of only 20.89% ($V_{oc}=2.33$ V, $J_{sc}=9.97$ mA. cm^{-2} FF=89.62%). when the other cell had a significantly improved PCE of 18.63%, with a V_{oc} of 1.78 V, and a J_{sc} of 12.48 mA. cm^{-2} and a FF of 83.72%.

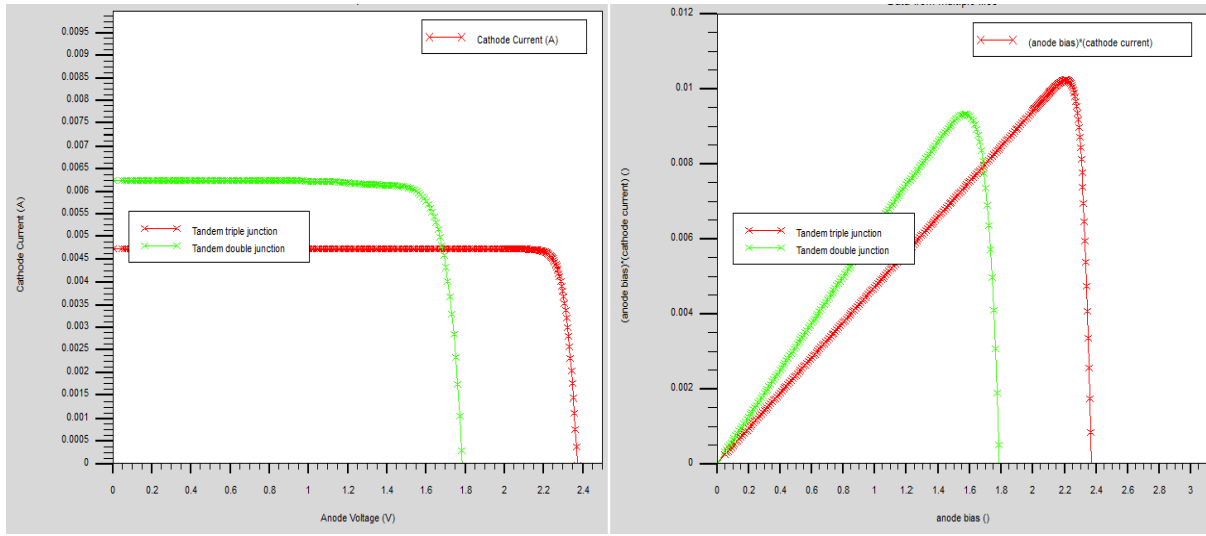


Fig.6. I-V and P-V Characteristics Overly of the double and triple solar cell.

4. Conclusion

In summary, we fabricated 20.89% efficient monolithic triple-junction solar cells by combining layers $Cu In_{1-x}Ga_xSe_2$ with band gaps of 1.67, 1.39 and 1.011 eV in a tandem with the middle sub-cell, we can achieve a better spectrum coverage leading to significantly improved V_{oc} and FF better than monolithic double-junction. Nevertheless, there remain challenges that need to be addressed to leverage the full potential of CIGS triple junction solar cells. Overall, we here demonstrate that high-performance $Cu In_{1-x}Ga_xSe_2$ triple-junction solar cell can be fabricated given the explosion of interest and rapid progress in multi-junction solar cells.

5. References

- [1] Yamaguchi, M., Takamoto, T., Araki, K. & Ekins- Daukes, N. (2003). III-V compound multi-junction solar cells: present and future. *Solar Energy Materials and Solar Cells*. 75(1), 261-269.
- [2] Guo, Y.Liang, Q. Shu Bifen. W, Jing.Yang, Q.The III-V triple-junction solar cell characteristics and optimization with a fresnel lens concentrator.*International Journal of*

Photoenergy. Hindawi Volume 2018, Article ID 7285849, <https://doi.org/10.1155/2018/7285849>.

[3] Xiao, K.Wen, J. Han, Q.Lin, R. Gao, Y.Gu, S. Zang, Y. Nie, Y.Zhu, J. Xu, J. Tan, H.Solution-Pprocessed monolithic all-perovskite triple-junction solar cells with efficiency exceeding 20.ACS Energy Letters,vol 5(2020), No. 2819- 2826 doi 10.1021/acseenergylett.0c01184.

[4] Bett, A.W., Dimroth, F., Guter, W., Hoheisel, R., Oliva, E., Philipps, S.P., Schone, J., Siefert, G., Steiner, M., Wekkeli, A., Welsler, E., Meusel, M., Kostler, W. & Strobl, G. (2009). Highest Efficiency Multi-Junction Solar Cell for Terrestrial and Space Applications. 24th European Photovoltaic Solar Energy Conference and Exhibition (PVSEC), Hamburg, Germany, pp1-6.

[5] Baur, C., Khorenko, V., Siefert, G., Bourgoin, J.C., Casale, M., Campesato, R., Duzellier, V. & Inguibert, V. (2013). Development Status of Triple-junction Solar Cells Optimized for Low Intensity Low Temperature Applications. 39th IEEE Photovoltaic Specialists Conferences (PVSC), TAMPA, United States, pp3237-3242.

a. Bounouh, G. Almuneau, H. Baumgartner, A. Cuenat, N. Gambacorti, J. Hoffmann, R. Kern, F. Kienberger, J. Krupka, D. Lackner, B. Pollakowski, T. G. Rodríguez, F. Sametoglu, L. Usydus, S. Winter, and F. Witt, 2014, The EMRP project Metrology for III-V materials based high efficiency multi-junction solar cells, CPEM 2014, IEEE Xplore, 318 – 319, DOI: 10.1109/CPEM.2014.6898387.

[6] Aho, A.Isoaho, R. Raappana, M. Aho, T.Anttola, E. Lyytiäinen, J.Hietalahti, A. Polojärvi, V. Tukiainen, A. Reuna, J. Peltomaa, L.Guina, M.Wide spectral coverage (0.7–2.2 eV) lattice-matched multijunction solar cells based on AlGaInP, AlGaAs and GaInNAsSb materials.Progress in Photovoltaics: Research and Applications.vol.29.NO.7.doi,<https://doi.org/10.1002/pip.3412>.

[7] J. Ivari, "A Paradigmatic Analysis of Contemporary Schools of IS Development", European Journal of Information Systems, Vol. 1, No. 4, 1991, pp. 249-272.

[8] T. Takamoto T. ,T. Agui , A. Yoshida, K. Nakaido , H. Juso, K. Sasaki , K. Nakamora, H. Yamaguchi,T. Kodama, H. Washio.

[9] M. Imaizumi .World's highest efficiency triple-junction solar cells fabricated by inverted layers transfer process. 2010 35th IEEE Photovoltaic Specialists Conference, 2010, pp. 000412-000417, doi: 10.1109/PVSC.2010.5616778.

[10] Dimroth, F., Guter, W., Schone, J., Welsler, E., Steiner, M., Oliva, E., Wekkeli, A., Siefert, G., Philipps, S.P., & Bett, A.W. (2009). Metamorphic GaInP/GaInAs/Ge triple-junction solar

cells with \gg 41 % efficiency. 2009 34th IEEE Photovoltaic Specialists Conference (PVSC), 001038-001042.

[11] Müller, R. Lackner, D.Höhn, O.Hauser, H. Bläsi, B. Predan, F. Benick, J. Hermle, M. Glunz, S W. Dimroth, F.Two-terminal III– V//Si triple-junction solar cell with power conversion efficiency of 35.9 % at AM1.5.(2022). *Progress in Photovoltaics: Research and Application*.Vol.30.No .869-879.

[12] Mufti, N., Amrillah, T., Taufiq, A., Sunaryono, Aripriharta, Diantoro, M., Zulhadjri, & Nur, H. (2020). Review of CIGS-based solar cells manufacturing by structural engineering. *Solar Energy*, 207(April), 1146–1157. <https://doi.org/10.1016/j.solener.2020.07.065>.

[13] Wei, Su Huai, S. B. Zhang, and Alex Zunger. 1998. “Effects of Ga Addition to CuInSe2 on Its Electronic, Structural, and Defect Properties.” *Applied Physics Letters* 72(24): 3199–3201.

[14] Jackson, P., Hariskos, D., Wuerz, R., Kiowski, O., Bauer, A., Friedlmeier, T. M., & Powalla, M. (2015). Properties of Cu(In,Ga)Se₂ solar cells with new record efficiencies up to 21.7%. *Physica Status Solidi - Rapid Research Letters*, 9(1), 28–31. <https://doi.org/10.1002/pssr.201409520>.

[15] Wang, Y. C., & Shieh, H. P. D. (2014). Double-graded bandgap in Cu(In,Ga)Se₂ thin film solar cells by low toxicity selenization process. *Applied Physics Letters*, 105(7), 0–4. <https://doi.org/10.1063/1.4893713>.

[16] Yamaguchi, Masafumi, Frank Dimroth, John F. Geisz, and Nicholas J. Ekins-Daukes. 2021. “Multi-Junction Solar Cells Paving the Way for Super High-Efficiency.” *Journal of Applied Physics* 129(24).

[17] Kadi, O., B. Dennai, and A. Laoufi. 2021. “Numerical Simulation of the Effect of Varied Buffer Layers on the Performance of Cu(In, Ga)Se₂ Solar Cells Using Silvaco Tcad 2D.” *Journal of Ovonic Research* 17(3): 247–51.

[18] Laoufi, A M., B. Dennai, Kadi, O. 2021. “Numerical Modeling of Multi-Junction Solar Cell-Based CIGS with Two Sub-Cells in Parallel Using Silvaco TCAD.” 18(6): 297–301.

[19] Boukortt, N. E. I., Patanè, S. & Abdulraheem, Y. M. Numerical investigation of CIGS thin-film solar cells. *Sol. Energy* 204, 440– 447 (2020).

[20] H. Amar and S. Tobbeche, “Study of electrical characteristics of CdS/CIGS (cadmium-sulfide/copper-indium-gallium-selenium) heterojunction solar cell,” no. May, pp. 4–5, 2015.

[21] F. Oliva, “Modelling, characterization and optimization of heat treatment processes for the formation of CIGS absorbers To cite this version: HAL Id: tel-01502706 ” 2017